



Preparation of Small-Molecule Microarrays by *trans*-Cyclooctene Tetrazine Ligation and Their Application in the High-Throughput Screening of Protein–Protein Interaction Inhibitors of Bromodomains**

Chong-Jing Zhang, Chelsea Y. J. Tan, Jingyan Ge, Zhenkun Na, Grace Y. J. Chen, Mahesh Uttamchandani, Hongyan Sun, and Shao Q. Yao*

The ϵ -N-acetylation of lysine residues (Kac) is one of the most common posttranslational modifications in proteins that are associated with epigenetics, and frequently occurs in large macromolecular complexes that play a role in chromatin remodelling, DNA damage, and cell-cycle control.^[1] In histones, acetylated lysines reduce electrostatic interactions with the negatively charged DNA phosphates, thus providing a more relaxed chromatin structure, which is associated with transcriptionally active genes. The cellular histone acetylation levels are strictly controlled by histone acetyltransferases (HATs; epigenetic “writers”) and histone deacetylases (HDACs; epigenetic “erasers”).^[2,3] Furthermore, Kac affects gene transcription through interactions with bromodomain (BRD)-containing proteins (BCPs; epigenetic “readers”).^[3,4] HATs and HDACs have traditionally been the main research focus in medicinal chemistry and drug discovery for epigenetic diseases.^[3,5] As enzymes, they are considered as “druggable”. The development of protein–protein interaction (PPI) inhibitors that target the epigenetic readers, on the other hand, is much more challenging. It is generally believed that small molecules do not bind sufficiently tightly to the much larger protein–protein interface because they contain only a limited number of functional groups.^[6] Such simplistic views, however, have recently been challenged by two ground-breaking studies that showed that certain benzodiazepine-containing compounds (e.g., **JQ1** and I-BET) are specific nanomolar PPI inhibitors of BET bromodomains (e.g., BRD4).^[7] This has spurred interest in compounds that might possess similar biological activities against other

BRDs.^[8] However, there remains a lack of sensitive assays for rapid and high-throughput screening (HTS) of other BRD-binding compounds. Existing assays, including those based on fluorescence polarization (FP), isothermal titration calorimetry (ITC), protein stability shift, and surface plasmon resonance (SPR), are either applicable to only a few well-known BRDs (e.g., BRD2/3/4), or they suffer from limited throughput because large amounts of proteins are required.^[9] Furthermore, for most of the 61 human BRDs, their cognate Kac-binding sequences are not well-understood. Recent large-scale structural studies and histone–peptide membrane arrays failed to identify any sub-micromolar-binding acetylated peptides that could be suitable for HTS assays.^[10] It is perhaps not surprising that both **JQ1** and I-BET were serendipitously discovered by HTS of random in-house compound libraries using cell-based reporter assays without any prior target information.^[7] These assays, though useful in their own right, are not target-oriented, and compounds identified during these assays may not actually act on their intended BRDs. Therefore, a prerequisite for drug-development efforts that focus on the discovery of new BRD inhibitors is the development of an HTS platform that is capable of general, rapid, and systematic large-scale screening of the interactions between BRDs and small molecules.

We recently developed a powerful small-molecule microarray (SMM) that is capable of sensitive, quantitative, and rapid identification of cell-permeable small-molecule PPI inhibitors.^[11] SMMs are miniaturized assemblies of small molecules that are immobilized across a planar glass slide, on which thousands of protein–ligand interactions (strong and weak) may be measured, with minimal consumption of proteins and ligands (in the nL to μ L range).^[12] We reasoned that BRDs, which are protein-binding domains that normally bind to cognate acetylated peptides with moderate or weak affinities, would be well-suited for our SMM approach. Herein, in a proof-of-concept study, we have successfully constructed a SMM on which 48 different benzodiazepines that are based on the core structure of **JQ1**/I-BET were immobilized, and screened it against 55 fluorescently labeled proteins, twelve of which were human BRDs (Figure 1). Specifically, we have 1) developed the first SMM that is based on bioorthogonal *trans*-cyclooctene (TCO) tetrazine ligation for site-specific covalent immobilization of TCO-modified benzodiazepines with unprecedented speed; 2) used this SMM for miniaturized HTS of these compounds against

[*] C.-J. Zhang, C. Y. J. Tan, Dr. J. Ge, Z. Na, G. Y. J. Chen, Dr. M. Uttamchandani, Prof. Dr. S. Q. Yao
Department of Chemistry, National University of Singapore
3 Science Drive 3, Singapore 117543 (Singapore)
E-mail: chmyaosq@nus.edu.sg
Homepage: <http://staff.science.nus.edu.sg/~syao>

Prof. Dr. H. Sun
Department of Biology and Chemistry, City University of Hong Kong
Hong Kong (P.R. China)

[**] Funding was provided by the National Medical Research Council (CBRG12nov100) and the Ministry of Education (MOE2012-T2-1-116 and MOE2012-T2-2-051). We also acknowledge a generous donation of bromodomain plasmids from Dr. James E. Bradner (Harvard Medical School) and Dr. Stefan Knapp (Oxford).



Supporting information for this article is available on the WWW under <http://dx.doi.org/10.1002/anie.201307803>.

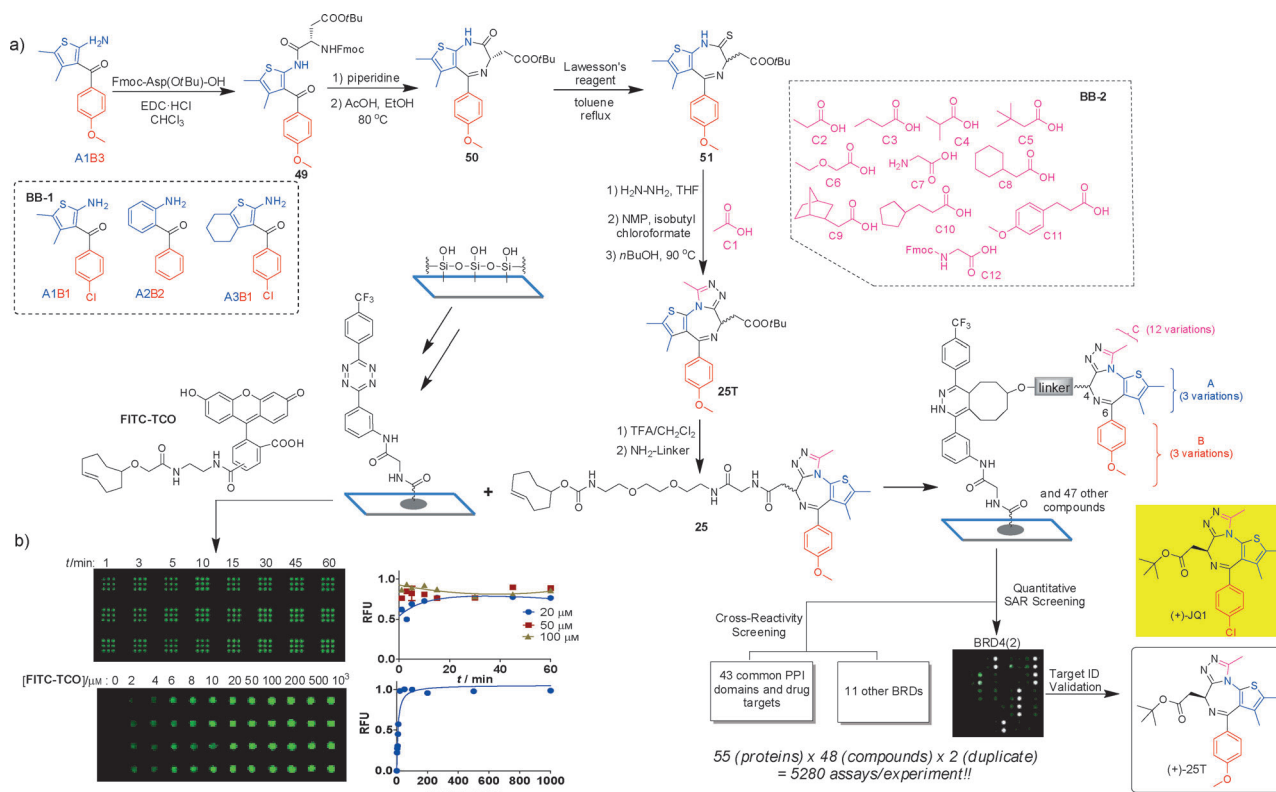


Figure 1. a) Synthesis of small molecules with a *trans*-cyclooctene tag (SM-TCO), followed by immobilization of SM-TCO onto tetrazine-functionalized slides to generate the corresponding SMMs; these were subsequently screened against fluorescently labeled proteins, including 12 BRDs and 43 other common PPI domains. The newly identified (+)-25T is shown, together with (+)-JQ1 (yellow box) and FITC-TCO, which was used as a positive spotting control. b) Assessment of the time- and concentration-dependence of the *trans*-cyclooctene tetrazine method for SMM immobilization. FITC-TCO (0–100 μM in a 1:1 DMSO/water solution) was used for spotting. Microarray results (left) were quantified and plotted (right). Fmoc = 9-fluorenylmethoxycarbonyl, NMP = *N*-methylpyrrolidine, SAR = structure–activity relationship, TFA = trifluoroacetic acid.

a variety of BRD and non-BRD proteins, including SH2 domains, 14-3-3, and other proteins, and established their cross-reactivity profiles; 3) discovered (+)-25T, a compound that possesses biological activities comparable to those of (+)-JQ1 in targeting BET bromodomains; and 4) discovered certain tetrazine-TCO-ligated products, for example, TT-1/3, that are strong binders of CREBBP and GCN5L2, which are non-BET BRDs.

A key step of SMM fabrication is the site-specific covalent immobilization of compound libraries with high efficiency.^[12] This is critical for the study of moderate or weak PPIs, such as those between BRDs and their ligands, for example, between acetylated peptides and benzodiazepines. Although many small-molecule immobilization methods have been developed over the years,^[12,13] none of them employs a covalent, site-specific, instantaneous, and chemoselective reaction under aqueous conditions to afford the highest possible concentration of immobilized ligand. Our previously developed strategy of using the biotin–avidin interaction for compound immobilization met some of these requirements,^[11,14] but failed to provide sufficiently intense signals for fluorescence detection (not shown), which is likely due to low compound loading of the surface. Most conventional bioorthogonal coupling reactions suffer from slow kinetics,^[15] including the Staudinger ligation ($k \approx 0.002 \text{ M}^{-1} \text{ s}^{-1}$), strain-promoted

alkyne–azide cycloadditions (SPAAC; $k \approx 1 \text{ M}^{-1} \text{ s}^{-1}$), and even the tetrazine norbornene ligation ($k \approx 1–2 \text{ M}^{-1} \text{ s}^{-1}$); when these transformations are used for microarray immobilization, they also require relatively long incubation times (2–24 h).^[13,16] This may lead to solvent evaporation, compound precipitation, and ultimately a decrease in immobilization efficiency.^[12]

To overcome these problems, we turned to the coupling of *trans*-cyclooctene (TCO) and tetrazine.^[17] With a second-order rate constant that exceeds $10^4 \text{ M}^{-1} \text{ s}^{-1}$, it is the fastest bioorthogonal reaction known. Although this reaction has been widely used in bioimaging,^[17a,b] material chemistry,^[17c] and activity-based protein profiling,^[17d] to the best of our knowledge, it has not been used for the construction of microarrays, including SMMs. The most closely related transformation that has been applied for such a process is the above-mentioned tetrazine norbornene ligation for the preparation of a carbohydrate microarray, which was described by Wittmann et al.,^[16] and which took 24 h to reach complete compound immobilization. In our current study, we prepared tetrazine-functionalized slides by sequential modifications of plain glass slides with (aminopropyl)triethoxysilane, succinic anhydride, and *N*-hydroxysuccinimide, followed by treatment with compound 56 (Supporting Information, Scheme S1) to give the surface shown in Figure 1 a. We next

spotted **FITC-TCO** (a model compound) to assess the efficiency of the immobilization of TCO-modified small molecules on these tetrazine slides (Figure 1b); time- and concentration-dependent results both indicate that the immobilization reaction was extremely rapid and highly efficient, with near-saturation of the **FITC-TCO** fluorescence observed within 1–5 min, even at a low spotting concentration (20 μM). This unprecedented rate for site-specific covalent immobilization of small molecules in a microarray nearly rivals that of the non-covalent biotin-avidin method ($k_{\text{on}} \approx 10^5\text{--}10^6 \text{M}^{-1} \text{s}^{-1}$),^[18] but this process affords a significantly higher immobilized-ligand concentration (data not shown).

Upon successful demonstration of this new immobilization method, we next focused on SMM construction. We synthesized a total of 48 different TCO-modified benzodiazepines, with structural variations at three key points of the core pharmacophore (**A**, **B**, **C**; Figure 1a). Based on the published X-ray structures of (+)-**JQ1** and the BRD4(2) complex (Figure S1),^[7a] the substituents at the C6 position (red) and on the triazole (purple) and thiophene (blue) rings in (+)-**JQ1** engage in critical interactions with the residues located in the Kac-binding pocket of BRD4(2). The compounds were synthesized over five steps by known procedures^[7] with suitable modifications (Figure 1a; see also the Supporting Information). In this synthesis, the acid-sensitive TCO was strategically introduced at the last step to ensure that its integrity was not compromised during the synthesis, and to simultaneously obtain TCO-free ligands, such as (+)-**25T**, which are needed for post-SMM validation experiments.

A total of 50 samples, including **1–48**, TCO-OH (**57**), and DMSO, were spotted in duplicate, as 12 identical sub-grids on single-tetrazine-functionalized glass slides, and simultaneously screened against different fluorescently labeled proteins at uniform concentration (1 μM). In total, 5280 PPI events with 55 different proteins (including 12 human BRDs, 39 SH2 domains, and 4 human 14-3-3 proteins, with the latter two classes being common phosphorylation readers) against all 48 benzodiazepines were delineated within hours in a single experiment by using five slides. The corresponding binding fingerprints are displayed in a color-coded heat map (Figure 2a), and representative microarray images are shown in Figure 2b. In general, weak or no binding between the immobilized compounds and non-BRD proteins was observed (Figure 2b; PLCG 1(C) and PLCG 1(N), from two SH2 domains). This indicates that the pharmacophore in **JQ1** and related benzodiazepines is indeed highly selective towards BRDs, as was previously observed.^[7] To our surprise, almost all immobilized compounds, including TCO-OH, showed nearly equal and strong fluorescent-ligand binding towards two non-BET BRDs, namely GCN5L2 and CREBBP, in a concentration-dependent manner (Figure 2b; see also Figure S7). This indicates that these bindings are likely to be specific. In the meantime, we carried out concentration-dependent microarray K_d determination against all 12 BRDs (Figure 2c and Figure S6), and the results were further extrapolated to obtain the corresponding *app* K_d (*app* K_d = apparent K_d ; Figure 2d).^[19] By comparing the *app* K_d of **13**, which is the SMM-immobilized form of **JQ1**,

against the published K_d of **JQ1**, which was measured by ITC experiments,^[7a] we found reasonably good correlations. For example, the *app* K_d values of the **13**/BRD4(1) and **13**/BRD4(2) interactions were shown to be $59.4 \pm 20.4 \text{ nm}$ and $131.5 \pm 35.4 \text{ nm}$, respectively, which are similar to the values reported ($49.0 \pm 2.4 \text{ nm}$ and $90.1 \pm 4.6 \text{ nm}$). We further showed that this SMM is highly sensitive, as it is capable of detecting strong BRD-binding ligands at protein concentrations as low as 10 nM (panel 1, Figure 2c). This indicates that our platform is indeed suitable for sensitive, rapid, semi-quantitative, and high-throughput K_d determination of BRD–ligand interactions. Dual-color ratiometric screening, in which two proteins, each labeled with a spectrally distinct fluorophore, are mixed in equal concentrations and simultaneously applied on the same microarray, enables rapid identification of isoform-specific ligands.^[14] Herein, we showed that this process can be used to discriminate between BET bromodomains (e.g., BRD2-4, BRDT) and other BRDs (e.g., PCAF, TAF1L, WDR9). BRD4(2)-specific ligands, including **1**, **13**, **25**, and **37**, could be visually identified (boxed red spots, Figure 2e). A selectivity score of $\log_2(\text{Cy5-Brd4(2)}/\text{Cy3-BRDx})$ was obtained for these compounds against all other BRDs (right graph; Figure 2e).

Previously, the enantiomerically pure (+)-**JQ1** was found to possess promising antitumor activities in cellular assays and animal models.^[7a] It also down-regulates the transcription of c-Myc (a well-known oncogene that plays a central role in the pathogenesis of cancer), which subsequently causes genome-wide down-regulation of Myc-dependent target genes.^[20] Aside from **13** (TCO-containing **JQ1**), we have identified several other potent and specific binders of BET bromodomains, including **1**, **25**, and **37**, by the SMM screening. We were particularly interested in compound **25**, as it was the most potent in terms of the binding to BRD4(2) (*app* K_d = $92.38 \pm 31.9 \text{ nm}$; Table S2), and it is a close structural analogue of **JQ1** (Figure 1). We therefore prepared its TCO-free enantiomerically pure versions, (+)-**25T** and (–)-**25T**, and tested their cellular activities (Figure 3a). Both (+)-**25T** and (+)-**JQ1** potently inhibited the growth of MV4-11 (B-myelomonocytic leukemia) and THP-1 (acute monocytic leukemia) cells in a dose-dependent manner, with comparable GI_{50} values ($95 \pm 0.9 \text{ nm}$ and $39 \pm 6.8 \text{ nm}$ for (+)-**25T** and (+)-**JQ1**, respectively; for the THP-1 results, see Figure S11). Compound (–)-**25T**, on the other hand, showed no activity at all. In a fluorescence-activated cell sorting (FACS) experiment, cells treated with both (+)-**25T** and (+)-**JQ1** showed an increase in the percentage of G0/G1 cells (Figure 3b). Finally, (+)-**25T**, similar to (+)-**JQ1**, was able to inhibit c-Myc expression in a both time- and concentration-dependent manner (Figure 3c). Taken together, these results indicate that (+)-**25T**, a compound identified from our newly developed SMM, is indeed a potent inhibitor of BET bromodomains and possesses cellular activities comparable to those of (+)-**JQ1**.^[7a,20]

Earlier, we unexpectedly observed that all of the TCO-immobilized spots on the SMM, including that of TCO-OH itself, produced strong and concentration-dependent fluorescent-ligand binding that was selective for two of the 12 BRDs screened, namely GCN5L2 and CREBBP (Figure 2 and

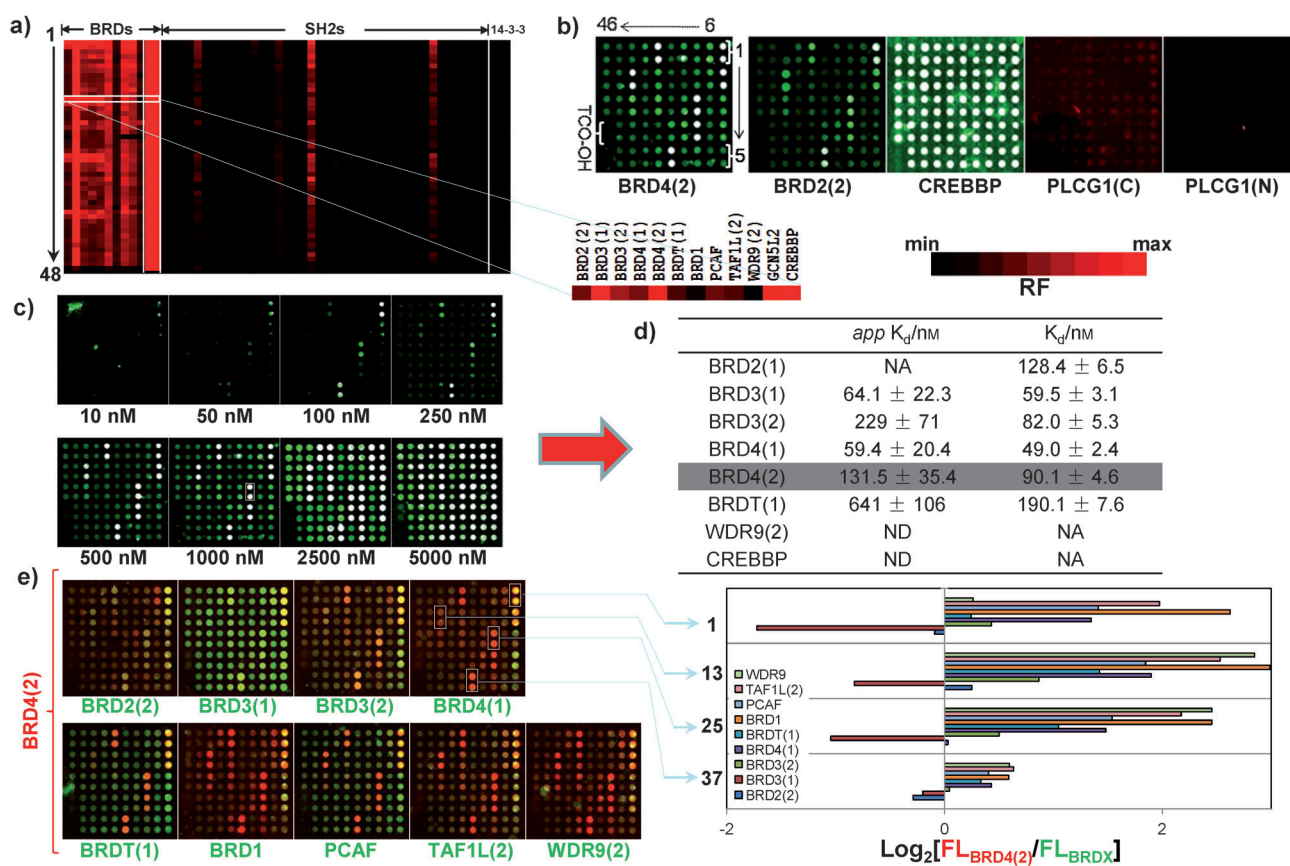


Figure 2. SMM screening results with different fluorescently labeled proteins, including 12 human BRDs. a) Color heat map displaying the binding of the 48 compounds with 55 fluorescently labeled proteins (1 μM), with highlighted rectangles showing the binding profiles of **13** with 12 BRDs (horizontal), and of all 48 compounds with GCN5L2 and CREBBP (vertical). **13** is the racemic form of TCO-containing **JQ1**. b) Microarray images that show the different binding profiles of representative proteins. All compounds were spotted in duplicate (vertical), and in a top-to-bottom and right-to-left manner (see the Supporting Information, Table S1 and S2). TCO-OH (**57**) and DMSO were spotted at positions 49 and 50, respectively. PLCG1(C) & PLCG1(N) are two representative SH2 domains. c) Concentration-dependent SMM-based K_d determination of the 48-member library against fluorescently labeled BRD4(2) (10–5000 nM). The spots corresponding to **13** are highlighted (box; 1000 nM image). d) Comparison of SMM-determined *app* K_d of **13T** against selected BRDs (extrapolated from Figure 2c) versus K_d values reported in the literature.^[7a] e) Merged microarray images of dual-color SMM screening results by using an equal mixture of Cy5-labeled BRD4(2) (500 nM; pseudo-colored in red) and another bromodomain (BRDX) that was labeled with Cy3 (500 nM; pseudo-colored in green). Selected spots (**1**, **13**, **25**, and **37**) were highlighted (in boxes). On the right side, a bar graph shows the selectivity scores, $\log_2(\text{Cy5-BRD4(2)}/\text{Cy3-BRDX})$, of selected compounds. A score of "0" indicates no selectivity, and "+" indicates BRD4(2)-preferred ligands. ND=not determined, NA=not available.

Figure S7). A plausible explanation is that these spots have a common structural motif that does not originate from the benzodiazepines. We speculate that the conjugate produced by TCO tetrazine ligation (Figure 3d) might constitute such a novel binder toward GCN5L2 and CREBBP. Both GCN5 (a histone acetyltransferase) and CREBBP (a protein that binds to the transcriptional activator CREB) are important cellular proteins. For the non-BET bromodomains within these proteins, only few small-molecule binders have been identified thus far.^[8c,21] To test whether compounds such as **TT-1/2/3**, in which the R group on one of the aromatic substituents of the tetrazine was varied, could positively bind to CREBBP and GCN5L2, ITC experiments were carried out (Figure S12); the results confirmed that all three compounds bind to both BRDs with K_d values in the low-micromolar region. We also synthesized **FTT** (inset, Figure 3d), a fluorescein derivative of **TT-2**, and confirmed its binding to GCN5L2 and CREBBP by fluorescence polarization. These

findings are interesting, as they indicate that **TT-1/2/3** are novel BRD-binding pharmacophores for GCN5 and CREBBP, and that **FTT** may serve as a good FP probe for HTS of potential GCN5/CREBBP inhibitors in the future.^[9] However, as other proteins could also bind to the TCO linker, we would like to point out that future SMM screenings using our platform should always be carried out with control spots that contain only TCO.

In conclusion, the bioorthogonal coupling between *trans*-cyclooctene (TCO) and tetrazine was shown to be exceedingly useful for the construction of small-molecule microarrays, and to afford immobilized ligands with unprecedented speed and surface concentration. By using this new chemoselective and covalent immobilization method, we have constructed the first benzodiazepine SMM suitable for miniaturized and high-throughput studies of potential PPI inhibitors against a variety of human bromodomains. We have identified (+)-**25T**, a structural analog of (+)-**JQ1**, as a potent

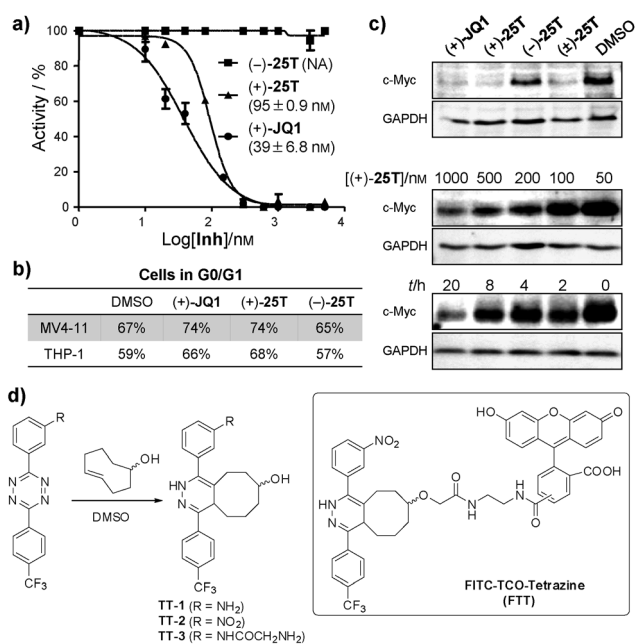


Figure 3. a) Dose-response growth curves of MV4-11 cells treated with (+)-JQ1, (+)-25T, or (-)-25T for 72 h. b) FACS results of MV4-11 cells upon treatment with DMSO, (+)-JQ1, (+)-25T, or (-)-25T (500 nM) for 24 h. The numbers denote the percentage of cells in the G0/G1 phase. c) Western blot analysis of c-Myc expression in MV4-11 cells upon treatment with different compounds. MV4-11 cells were treated with each compound (500 nM) or DMSO for 24 h (Top image). Concentration- (middle) and time-dependent (bottom) c-Myc expression in MV4-11 cells that were treated with (+)-25T. d) Structures of TT-1/2/3, which were obtained by ligation between the three structurally different tetrazines and TCO-OH, and the FP probe FTT (box). NA = not available.

inhibitor for BET bromodomains, both in vitro and in cell-based assays. During the course of our study, we unexpectedly discovered that the ligation products of TCO and tetrazine, namely TT-1/2/3, relatively strongly and selectively bind to bromodomains of CREBBP and GCN5. The corresponding fluorescein-functionalized compound (FTT) may be used for HTS of potential PPI inhibitors in the future.

Received: September 5, 2013

Revised: September 30, 2013

Published online: November 4, 2013

Keywords: bioorthogonal chemistry · epigenetics · inhibitors · protein-protein interactions · small-molecule microarrays

- [1] a) S. L. Berger, *Nature* **2007**, *447*, 407–412; b) T. Kouzarides, *Cell* **2007**, *128*, 693–705.
 [2] K. K. Lee, J. L. Workman, *Nat. Rev. Mol. Cell Biol.* **2007**, *8*, 284–295.
 [3] C. H. Arrowsmith, C. Bountra, P. V. Fish, K. Lee, M. Schapira, *Nat. Rev. Drug Discovery* **2012**, *11*, 384–400.
 [4] A. C. Belkina, G. V. Denis, *Nat. Rev. Cancer* **2012**, *12*, 465–477.
 [5] a) S. Minucci, P. G. Pelicci, *Nat. Rev. Cancer* **2006**, *6*, 38–51; b) J. L. Duffner, P. A. Clemons, A. N. Koehler, *Curr. Opin. Chem. Biol.* **2007**, *11*, 74–82; c) A. J. Vegas, J. H. Fuller, A. N.

- Koehler, *Chem. Soc. Rev.* **2008**, *37*, 1385–1394; d) C. A. Hassig, S. L. Schreiber, *Curr. Opin. Chem. Biol.* **1997**, *1*, 300–308.
 [6] a) A. J. Wilson, *Chem. Soc. Rev.* **2009**, *38*, 3289–3300; b) M. R. Arkin, J. A. Wells, *Nat. Rev. Drug Discovery* **2004**, *3*, 301–317.
 [7] a) P. Filippakopoulos, J. Qi, S. Picaud, Y. Shen, W. B. Smith, O. Fedorov, E. M. Morse, T. Keates, T. T. Kickman, I. Felletar, M. Philpott, S. Munro, M. R. McKeown, Y. Wang, A. L. Christie, N. West, M. J. Cameron, B. Schwartz, T. D. Heightman, N. L. Thangue, C. A. French, O. Wiest, A. L. Kung, S. Knapp, J. E. Brandner, *Nature* **2010**, *468*, 1067–1073; b) E. Nicodeme, K. L. Jeffrey, U. Schaefer, S. Beinke, S. Dewell, C.-W. Chung, R. Chandwani, I. Marazzi, P. Wilson, H. Coste, J. White, J. Kirilovsky, C. M. Rice, J. M. Lora, R. K. Prinjha, K. Lee, A. Tarakhovskiy, *Nature* **2010**, *468*, 1119–1123.
 [8] For recent examples, see: a) C. W. Chung, A. W. Dean, J. M. Woolven, P. Bamborough, *J. Med. Chem.* **2012**, *55*, 576–586; b) D. S. Hewings, M. Wang, M. Philpott, O. Fedorov, S. Uttarkar, P. Filippakopoulos, S. Picaud, C. Vuppasetty, B. Marsden, S. Knapp, S. J. Conway, T. D. Heightman, *J. Med. Chem.* **2011**, *54*, 6761–6770; c) D. S. Hewings, O. Fedorov, P. Filippakopoulos, S. Martin, S. Picaud, A. Tumber, C. Wells, M. M. Olcina, K. Freeman, A. Gill, A. J. Ritchie, D. W. Sheppard, A. J. Russell, E. M. Hammond, S. Knapp, P. E. Brennan, S. J. Conway, *J. Med. Chem.* **2013**, *56*, 3217–3227.
 [9] C.-W. Chung, J. Witherington, *J. Biomol. Screening* **2012**, *16*, 1170–1185.
 [10] P. Filippakopoulos, S. Picaud, M. Mangos, T. Keates, J.-P. Lambert, D. Barsyte-Lovejoy, I. Felletar, R. Volkmer, S. Muller, T. Pawson, A.-C. Gingras, C. H. Arrowsmith, S. Knapp, *Cell* **2012**, *149*, 214–231.
 [11] H. Wu, J. Ge, S. Q. Yao, *Angew. Chem.* **2010**, *122*, 6678–6682; *Angew. Chem. Int. Ed.* **2010**, *49*, 6528–6532.
 [12] Y. M. Foong, J. Fu, S. Q. Yao, M. Uttamchandani, *Curr. Opin. Chem. Biol.* **2012**, *16*, 234–242.
 [13] a) H. Wu, J. Ge, M. Uttamchandani, S. Q. Yao, *Chem. Commun.* **2011**, *47*, 5664–5670; b) M. Uttamchandani, J. Wang, S. Q. Yao, *Mol. BioSyst.* **2006**, *2*, 58–68.
 [14] C. H. S. Lu, H. Y. Sun, F. B. Abu Bakar, M. Uttamchandani, W. Zhou, Y. C. Liou, S. Q. Yao, *Angew. Chem.* **2008**, *120*, 7548–7551; *Angew. Chem. Int. Ed.* **2008**, *47*, 7438–7441.
 [15] E. M. Sletten, C. R. Bertozzi, *Angew. Chem.* **2009**, *121*, 7108–7133; *Angew. Chem. Int. Ed.* **2009**, *48*, 6974–6998.
 [16] H. S. G. Beckmann, A. Niederwieser, M. Wiessler, V. Wittmann, *Chem. Eur. J.* **2012**, *18*, 6548–6554.
 [17] a) N. K. Devaraj, R. Upadhyay, J. B. Haun, S. A. Hilderbrand, R. Weissleder, *Angew. Chem.* **2009**, *121*, 7147–7150; *Angew. Chem. Int. Ed.* **2009**, *48*, 7013–7016; b) N. K. Devaraj, S. Hilderbrand, R. Upadhyay, R. Mazitschek, R. Weissleder, *Angew. Chem.* **2010**, *122*, 2931–2934; *Angew. Chem. Int. Ed.* **2010**, *49*, 2869–2872; c) J. B. Haun, N. K. Devaraj, S. A. Hilderbrand, H. Lee, R. Weissleder, *Nat. Nanotechnol.* **2010**, *5*, 660–665; d) K. S. Yang, G. Budin, C. Tassa, O. Kister, R. Weissleder, *Angew. Chem.* **2013**, *125*, 10787–10791; *Angew. Chem. Int. Ed.* **2013**, *52*, 10593–10597.
 [18] R. Y. P. Lue, G. Y. J. Chen, Y. Hu, Q. Zhu, S. Q. Yao, *J. Am. Chem. Soc.* **2004**, *126*, 1055–1062.
 [19] M. Uttamchandani, W. L. Lee, J. Wang, S. Q. Yao, *J. Am. Chem. Soc.* **2007**, *129*, 13110–13117.
 [20] J. E. Delmore, G. C. Issa, M. E. Lemieux, P. B. Rahl, J. Shi, H. M. Jacobs, E. Kastrits, T. Gilpatrick, R. M. Paranal, J. Qi, M. Chesi, A. C. Schinzel, M. R. McKeown, T. P. Heffernan, C. R. Vakoc, P. L. Bergsagel, I. M. Ghobrial, P. G. Richardson, R. A. Young, W. C. Hahn, K. C. Anderson, A. L. Kung, J. E. Bradner, C. S. Mitsiades, *Cell* **2011**, *146*, 904–917.
 [21] C. W. Chung, D. F. Tough, *Drug Discovery Today Ther. Strategies* **2012**, *9*, e111–120.